

B.A. NAJAFOV,¹ V.V. DADASHOVA²¹ Institute of Radiation Problems, Azerbaijan National Academy of Sciences
(9, Vakhazade Str., AZ1143 Baku, Azerbaijan; e-mail:
bnajafov@rambler.ru, bnajafov@physics.ab.az)² Baku State University
(23, Z/Khalilov Str., AZ1143 Baku, Azerbaijan)**OPTOELECTRONIC PROPERTIES
OF HYDROGENATED AMORPHOUS SILICON–CARBON
AND NANOCRYSTALLINE-SILICON THIN FILMS**PACS 78.40.Fy, 88.40.H-,
78.66.Db

Some parameters of thin films fabricated of hydrogenated amorphous silicon–carbon alloys $a\text{-Si}_{1-x}\text{C}_x\text{:H}$ with $x = 0$ and 0.5 and nanocrystalline silicon ($nc\text{-Si}$) and serving as a basis for developing solar cells including a Schottky barrier and $p\text{-i-n}$ and double $p\text{-i-n}$ heterojunctions have been considered. In double $p\text{-i-n}$ heterojunctions, $a\text{-SiC}/a\text{-Si}/nc\text{-Si}$, the p -layer was made from $a\text{-SiC:H}$ and used as a “window”, and the n -layer was made from $nc\text{-Si}$. The current-voltage characteristics of solar cells of each type at their illumination are studied. The highest efficiency of 11.5% was found for solar cells with the double $p\text{-i-n}$ heterojunctions in the case where a cell 1 cm^2 in area was illuminated with light of a 100-mW/cm^2 intensity.

Keywords: films of a hydrogenated amorphous silicon–carbon alloy, films of nanocrystalline silicon, plasma-chemical technique, crystallites, efficiency of solar cells.

1. Introduction

Films of the hydrogenated amorphous silicon–carbon alloy ($a\text{-Si}_{1-x}\text{C}_x\text{:N}$) and nanocrystalline silicon ($nc\text{-Si}$) are characterized by wider energy gaps and better optoelectronic properties in the visible spectral range in comparison with films of amorphous silicon. They are also more thermodynamically stable and radiation-resistant [1–3]. Those properties allow them to be used for the development of solar cells [4–7]. If comparing with the films of the $a\text{-Si:N}$ type, hydrogenated amorphous silicon–germanium alloys ($a\text{-Si}_{1-x}\text{Ge}_x\text{:N}$) have a narrower energy gap and low photoconducting properties. Therefore, $a\text{-Si}_{1-x}\text{C}_x\text{:N}$ films doped with phosphorus and boron, as well as $nc\text{-Si}$, are of larger interest than other silicon alloys.

Experiments show that amorphous films can be deposited onto various structural phases by varying technological parameters and conditions. In work

[4], the methods of x-ray diffraction and IR spectroscopy were used to study nanocrystalline SiC films $0.5 \div 1.0\ \mu\text{m}$ in thickness obtained by magnetron sputtering onto quartz substrates at a temperature of $200 \div 600\ \text{°C}$ in the 80% H_2 –20% Ar plasma. As the temperature was elevated from 300 to 600 °C, an increase in the density of SiC nanocrystals was observed, with the average size amounting to 5 nm. A similar result was also obtained in work [3] for nanocrystalline Si obtained using plasma-chemical deposition.

**2. Experimental Results
and Their Discussion**

In this work, we studied films of hydrogenated amorphous silicon–carbon alloy $a\text{-Si}_{1-x}\text{C}_x\text{:H}$ doped with boron and films of amorphous nanocrystalline Si doped with phosphorus (PH_3). The films of both kinds were obtained using the method of plasma-chemical deposition. The discharge power reached

20 ÷ 200 W, the substrate temperature was $T_S = 200 \div 300$ °C, the time of film deposition was 0.5 ÷ 1 h, the deposition rate changed within the limits of 3 ÷ 5 Å/s, and the film thickness was $d = 100 \div 7000$ Å. The gas consumption amounted to 0.5 ÷ 6.0 cm³/min at a pressure of $5 \times 10^{-3} \div 10^{-4}$ Torr. Before the deposition, the films were carefully treated chemically and degassed in vacuum at $T = 300$ °C. The design of an installation for the film fabrication was described in works [3, 8] in detail. Amorphous ternary alloys $a\text{-Si}_{1-x}\text{C}_x\text{H}$ were prepared from gas mixtures $\text{SiH}_4 + \text{CH}_4 + \text{H}_2$. Hydrogen was added in the following contents: $[\text{PH}_3/\text{SiH}_4]:\text{H}_2 = 1:20$ for n -type films and $[\text{B}_2\text{H}_6/\text{SiH}_4 + \text{CH}_4]:\text{H}_2 = 1:10$ for p -type ones.

By analyzing the halfwidth of x-ray lines (for diffraction peaks of reflection from planes $\langle 111 \rangle$, $\langle 220 \rangle$, and $\langle 311 \rangle$), the average size of crystallites, δ , was calculated. For films 50 nm² in area and doped with phosphorus, and provided the high-frequency discharge power $W_{\text{rf}} = 150$ W and the substrate temperature $T_S = 300$ °C, this parameter amounted to 8 nm (Fig. 1, curve 2). For undoped films 75 nm² in area, the dimensions of crystallites ranged up to 8 nm (Fig. 1, curve 3). For boron-doped films (B_2H_6) 30 nm² in area, the dimensions of crystallites amounted to 5 nm (Fig. 1, curve 1).

Films of nc-Si were fabricated at a higher discharge power of about 200 W and the substrate temperature $T_S = 300$ °C. Films deposited at discharge powers lower than 100 W gave the diffraction patterns typical of amorphous silicon, whereas films obtained at discharge powers more than 100 W gave the diffraction patterns typical of the amorphous-nanocrystalline phase. The average size of crystallites in each film was estimated according to the Debye-Scherrer relation for the diffraction line halfwidth.

The scattering of x-rays at the planes $\langle 111 \rangle$ of the silicon crystal lattice, the angular positions of $2\theta_p$ peaks, their height I_p , and halfwidth $\Delta(2\theta)$ were different for doped and undoped films. Assuming that the derivative of $I_p\Delta(2\theta)$ is proportional to the volume of the nanocrystalline phase X_c , the latter parameter for nc-Si films was determined after their deposition. The results obtained show that, in as-deposited undoped films, the fraction of the nanocrystalline phase in the amorphous matrix amounts to 70% of the whole film volume. In nc-Si films doped with phosphorus (PH_3), the total volume of crystallites amounted to 50% of the film volume and, in the

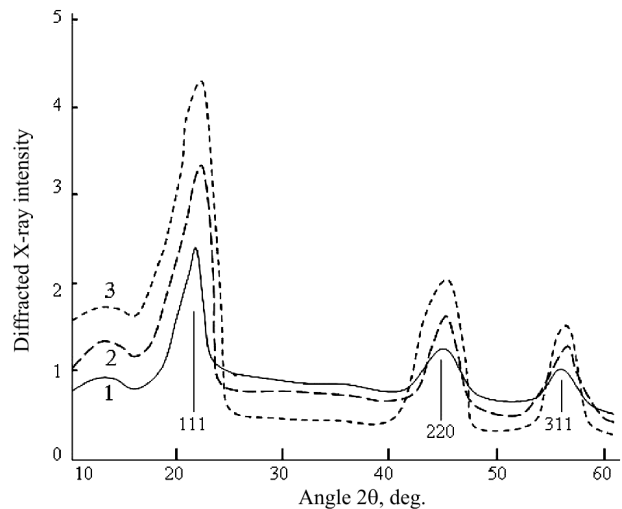


Fig. 1. Angular dependences of the x-ray scattering intensity I_x by nanocrystalline silicon: (1) boron-doped (B_2H_6), (2) phosphorus-doped (PH_3), and (3) undoped films after their deposition at the substrate temperature $T_S = 300$ °C

boron-doped nc-Si films, to 30%. Similar results were also observed for the planes $\langle 220 \rangle$ and $\langle 311 \rangle$ of the silicon crystal lattice. As the temperature grew in the course of the thermal treatment, the hydrogen effusion took place at 500 °C, and the hydrogen content in the undoped nc-Si film decreased from 24 to 8 at.% (Fig. 3). The results obtained are schematically exhibited in Fig. 2. At a further increase of the annealing temperature, the hydrogen content approached 1 at.%. The obtained results were verified by the method of IR absorption spectroscopy. On the basis of those results, we may assert that monohydride, Si-H, and dihydride, Si-H₂, complexes play the role of a spatial barrier in the film volume and affect the growth of nanocrystals [9].

3. Creation of Solar Cells

Solar cells on the basis of hydrogenated amorphous films $a\text{-Si:H}$ and their alloys were studied in a number of works [1–12]. Note that such alloys are characterized by two types of phases, amorphous and nanocrystalline, the most interesting being the phases that are located at the crystallinity boundary and considered to be the most stable for the creation of solar cells. To increase the photoconductivity, either hydrogen is introduced into the films or the latter are grown in a hydrogen environment. Cryst-

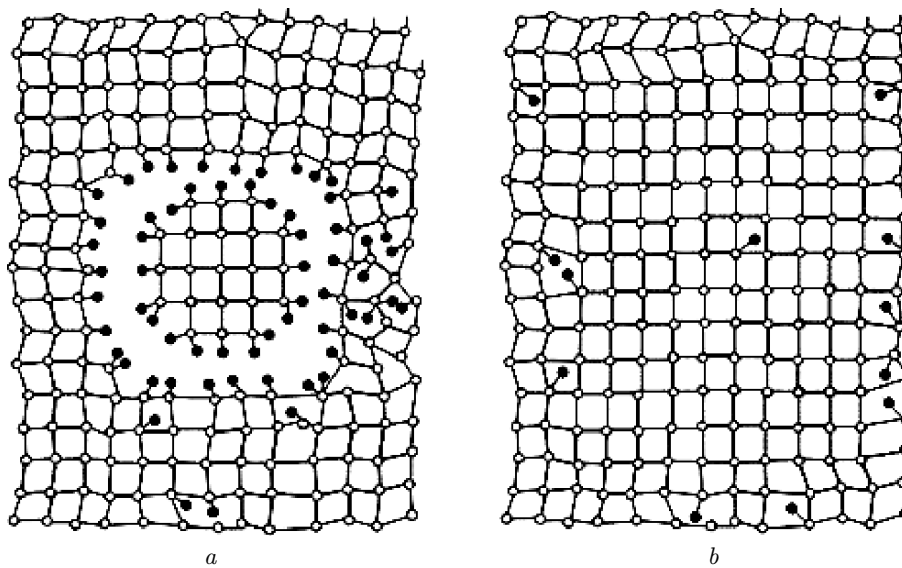


Fig. 2. Schematic models for *nc*-Si film structures (1) after the deposition and (2) after the annealing at $T_a \geq 600$ °C for $t = 1$ h

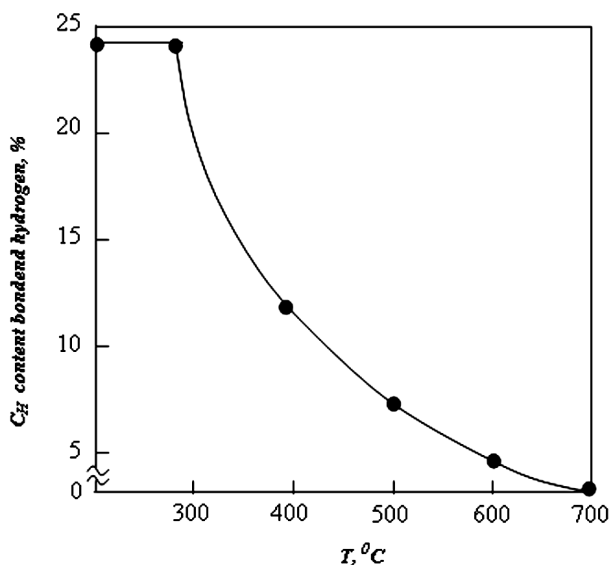


Fig. 3. Dependence of the hydrogen content in films on the annealing temperature T_a . Hydrogen content C_H , at.%

tallization improves the thermodynamic stability of the films, and hydrogenation improves the film quality. Thus, the task consists in the determination of an optimal regime for the film fabrication. For attaining the photogalvanic effect, the cells were illuminated with a light source of an intensity of about 100 mW/cm².

Solar cells with a double *n-i-p* heterojunction and the structure glass/indium and tin oxides (ITO)/*i*(*a*-Si:H)/*n*⁺(*nc*-Si) were fabricated as follows. A layer of boron-doped *a*-SiC:H of the *p*-type [$B_2H_6 : (SiH_4 + CH_4) = 0.1\%$] and 300 Å in thickness was deposited onto a transparent conducting ITO film preliminarily sputtered onto a glass substrate. Then, an undoped *i*-layer of *a*-Si:H with the thickness $d = 7000$ Å was deposited and covered by a phosphorus-doped *nc*-Si layer of the *n*-type ($PH_3 : SiH_4 = 0.5\%$) and with a thickness of 500 Å. At last, a contact made of Ti/Ag alloys was deposited. The coefficient of optical absorption α for the *i*-layer in the visible spectral range reached 5×10^4 cm⁻¹ and was described by the relation

$$\sqrt{\alpha h\nu} = B(h\nu - E_0), \tag{1}$$

where the coefficient $B = 539$ eV⁻¹cm^{-1/2} was determined by linearly extrapolating the dependence of the quantity $\sqrt{\alpha h\nu}$ on the photon energy $h\nu$, and $E_0 = 1.80$ eV is the energy gap width. If the “window” for the radiation withdrawal turns out too thin, the open-circuit voltage V_∞ increases. In the opposite case of a too thick “window”, the short-circuit current density I_{sc} increases. Therefore, we selected optimum thicknesses for the “windows”. In particular, the largest V_∞ and I_{sc} were obtained at a “window” thickness of 300 Å. This factor, in turn, governs

the cell efficiency. The maximum efficiency coefficient amounted to $\eta = 11.5\%$ at the short-circuit current density $I_{sc} = 17.0 \text{ mA/cm}^2$, the open-circuit voltage $V_\infty = 0.96 \text{ V}$, and the filling coefficient $\xi = 0.71$ (Fig. 4, curve 3).

Highly effective solar cells on stainless steel substrates and with the $n-i-p$ heterojunction structure $\text{ITO}/n^+(\text{nc-Si})/i(\text{a-Si:H})/p^+(\text{nc-Si})$ were fabricated analogously. Nanocrystalline films of $n^+(\text{nc-Si})$ doped with phosphorus and 500 \AA in thickness were deposited at a substrate temperature of $300 \text{ }^\circ\text{C}$ and a HF discharge power of 150 W . We prepared the $p^+(\text{nc-Si})$ layer of a thickness of 300 \AA ; then an n^+ -layer was deposited in the same reactor and under the same conditions. The i -layer thickness was $d = 5000 \text{ \AA}$. As a coating layer, we chose ITO with a light transmittance of 80% . Aluminum was used for the front contact and stainless steel for the rear one. The corresponding p^+ and n^+ layers were made with the use of the B_2H_6 and PH_3 gas mixture. Note that the ratio between the products $\mu\tau$ of the lifetime and the mobility for holes and electrons equals $\mu_p\tau_p/\mu_n\tau_n \approx 0.01$. The fabricated solar cells had the following characteristics: the short-circuit current $I_{sc} = 14.9 \text{ mA/cm}^2$, the open-circuit voltage $V_\infty = 0.92 \text{ V}$, the filling coefficient $\xi = 0.69$, and the efficiency $\eta = 9.45\%$ (Fig. 4, curve 2).

In order to improve the quality of a solar cell and the reproducibility of its work, the substrate was first covered with an n^+ -layer of nanocrystalline Si (300 \AA in thickness), then with an i -layer on the basis of a-Si:H (5000 \AA in thickness). The barrier was created by depositing a metallic (Pt) layer 100 \AA in thickness. Palladium was used for the front contact, and a steel substrate for the rear one. From the relation between I_{sc} and V_∞ ,

$$V_\infty = \frac{n'kT}{q} \ln \left(\frac{I_{sc}}{I_0} + 1 \right), \quad (2)$$

the diode quality factor was determined. For the Schottky barrier, $n-i-p$ -heterojunctions, and double heterojunctions, this quantity was found to equal $n' = 1.58, 1.82,$ and 2.1 , respectively [13, 14]. The saturation current density for the diodes was determined by the formula

$$I_0 = q\mu_c N_c E_c \exp \left(-\frac{\varphi_B}{kT} \right), \quad (3)$$

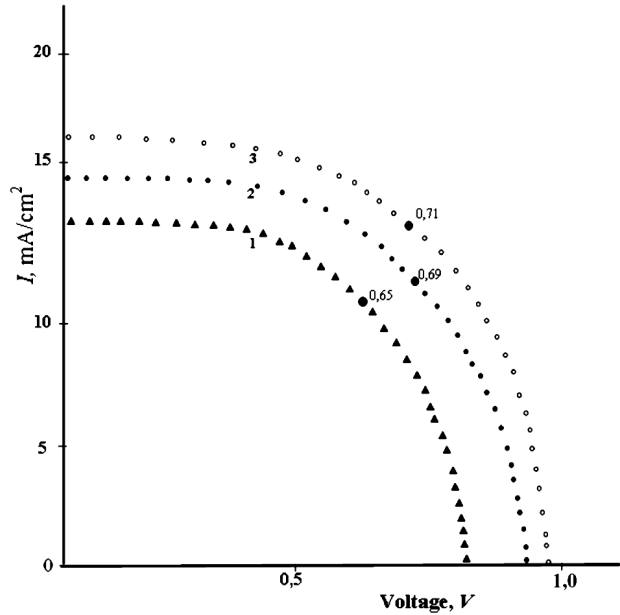


Fig. 4. Parameters of solar cells at an illumination power of 100 mW/cm^2 for the cells with the Schottky barrier (1), $n-i-p$ heterojunction (2), and double heterojunction (3)

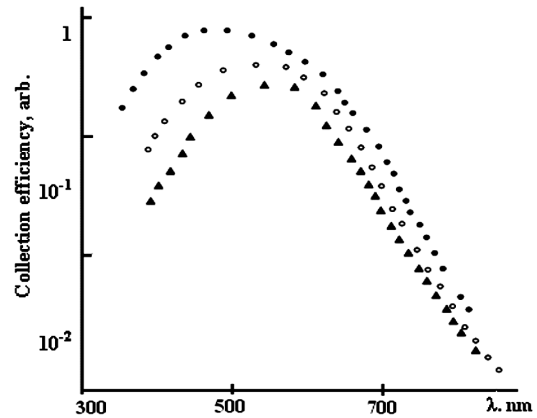


Fig. 5. Dependences of the collection efficiency on the incident light wavelength for solar cells with the Schottky barrier (\blacktriangle), $n-i-p$ heterojunction (\circ), and double heterojunction (\bullet)

where $\mu_c = 20 \text{ cm}^2/\text{V/s}$ is the mobility of an electron in the conduction band, $N_c = 10^{21} \text{ cm}^{-3} \text{ eV}^{-1}$ is the effective density of states in the conduction band, $E_c = 10^4 \text{ V/cm}$, and q is the electron charge [15]. The barrier height φ_B was determined from expressions (2) and (3),

$$V_\infty = \frac{n'kT}{8} [\ln I_{sc} - \ln (q\mu_c N_c E_c)] + n^I \varphi_B. \quad (4)$$

The curve of the temperature dependence of V_∞ intersects the ordinate axis ($T = 0$) at φ_B since $n^I \approx 1$. As a result, we obtain the value $\varphi_B = 1.1$ eV [13–15].

The capacity-voltage (C - V) characteristics [13, 14] were used to determine the value of intrinsic potential $V_0 = 0.42$ eV and the space charge density $N \approx 3 \times 10^{15}$ cm $^{-3}$. Then, an equation from work [13] rewritten in the form

$$W_e = (\varepsilon/2\pi q)^{1/2}(V_0/N)^{1/2}, \quad (5)$$

was used for the determination of the depleted layer width $W_e = 0.35$ μ m.

Curve 1 in Fig. 4 was used to determine the highest efficiency $\eta = 6.05\%$ and the best $I_{sc} = 12.1$ mA/cm 2 at $V_\infty = 0.77$ V and $\xi = 0.65$.

In Fig. 5, the dependences of the collection efficiency on the light wavelength measured at a photon flux of about $10^{17} \div 10^{18}$ m $^{-2}$ s $^{-1}$ and in the short-circuit mode are shown. The efficiency of charge carrier collection $Y(\lambda)$ at various wavelengths was determined as the ratio between the number of incident photons and the number of free carriers collected by the external circuit [16, 17],

$$Y(\lambda) = I_p(\lambda)/eN(\lambda), \quad (6)$$

where $I_p(\lambda) = 10$ mA/cm 2 is the photocurrent density, $N(\lambda)$ the flux of incident photons, and e the free carrier charge. In the case of photocurrent saturation, when all excited charge carriers are collected in the short-circuit mode, the measured collection efficiency does not depend on the reverse bias voltage. The observable shift of the maximum and a reduction of the collection efficiency in the long-wave spectral regions are explained by a decrease of the absorption factor α in the active i -layer, when the space charge expands over the solar cell volume, as well as by energy losses. When the elements were illuminated by light with a wavelength within the interval of $0.3 \div 0.9$ μ m and an intensity of 100 mW/cm 2 for 720 h, their photovoltaic properties did not reveal any changes in the cell parameters.

4. Conclusions

Amorphous hydrogenated ternary alloys a -Si $_{1-x}$ C $_x$:H doped with boron (B $_2$ H $_6$) and used as “windows” of the p -type and nanocrystalline silicon (nc -Si) doped with boron and phosphorus (PH $_3$) were deposited

with the use of the plasma-chemical technique under various technological conditions. By analyzing the halfwidth of x-ray lines, the average size of crystallites, δ , was calculated. For undoped as-deposited nc -Si films 75 nm 2 in area, this parameter amounted to 10 nm. For phosphorus- and boron-doped films 50 to 30 nm 2 in area, the average size of crystallites decreased from 8 to 5 nm, respectively. The presented results testify that a -Si $_{1-x}$ C $_x$:H and nc -Si films are promising objects for the creation of solar cells. The efficiency of solar cells 1.0 cm 2 in area was found to equal $\eta = 6.05\%$ for Schottky barriers, 9.45% for p - i - n heterojunctions, and 11.5% for double p - i - n heterojunctions.

1. *The Physics of Hydrogenated Amorphous Silicon II. Electronic and Vibrational Properties*, edited by J.D. Joannopoulos and G. Lukovsky (Springer, Berlin, 1984).
2. V.P. Afanasyev, A.S. Gudovskikh, V.N. Nevedomskii, and A.P. Sazonov, *Fiz. Tekh. Poluprovodn.* **36**, 238 (2003).
3. B.A. Najafov and V.R. Figarov, *Int. J. Hydrog. Ener.* **35**, 4361 (2010).
4. H. Colder, R. Rizk, M. Morales, P. Marie *et al.*, *J. Appl. Phys.* **98**, 543 (2005).
5. H. Zhihua, L. Xianbo, D. Hongwei, C. Shibin, Z. Yi, F. Elvira, and M. Rodrigo, *J. Non-Cryst. Solids* **352**, 1900 (2006).
6. B. Francesco and F. Enza, *Thin Solid Films* **33**, 34 (2003).
7. M.G. Park, W.S. Choi, B. Hong, Y.T. Kim *et al.*, *J. Vac. Sci. Technol. A* **20**, 861 (2002).
8. B.A. Najafov and G.I. Isakov, *Alternat. Energet. Ekolog.* **24**, 79 (2005).
9. B.A. Najafov, in *Proceedings of the 2-nd Republican Conference on Actual Problems in Physics* (Baku, Azerbaijan, 2008), p. 46 (in Russian).
10. M. Cardona, *Phys. Status Solidi B* **118**, 463 (1983).
11. B.A. Najafov, *Alternat. Energet. Ekolog.* **11**, 174 (2007).
12. D.J. Staebler, R.S. Crandall, and R. Williams, *Appl. Phys. Lett.* **39**, 733 (1981).
13. *Amorphous Semiconductors*, edited by M.H. Brodsky (Springer, Berlin, 1979).
14. B.A. Najafov and V.R. Figarov, *Int. J. Sustain. Ener.* **26**, No. 4, 7 (2007).
15. B.A. Najafov, *Fiz. Tekh. Poluprovodn.* **34**, 1383 (2000).
16. A. Madan and M. Shaw, *The Physics and Applications of Amorphous Semiconductors* (Boston, Academic Press, 1988).
17. B.A. Najafov and G.I. Isakov, *Neorg. Mater.* **45**, 711 (2009).

Received 23.11.12.

Translated from Ukrainian by O.I. Voitenko

Б.А. Наджафов, В.В. Дадашова

ОПТОЕЛЕКТРОННІ ВЛАСТИВОСТІ
ТОНКИХ ПЛІВОК ГІДРОГЕНІЗОВАНОГО
АМОРФНОГО КРЕМНІЮ-ВУГЛЕЦЮ
І НАНОКРИСТАЛІЧНОГО КРЕМНІЮ

Резюме

У роботі розглянуто деякі параметри тонких плівок гідрогенізованого аморфного сплаву кремнію-вуглецю ($a\text{-Si}_{1-x}\text{C}_x\text{:H}$) ($x = 0; 0,5$) і нанокристалічного кремнію

($nc\text{-Si}$). На основі цих плівок розроблено сонячні елементи з бар'єрами Шотткі, $n\text{-i-p}$ і подвійним $n\text{-i-p}$ гетеропереходом. Елементи подвійних гетеропереходів $a\text{-SiC}/a\text{-Si}/nc\text{-Si}$, в яких p -шар виготовлявся з $a\text{-SiC:H}$ і використовувався як "вікна", і n -шар виготовлявся з $nc\text{-Si}$. Досліджено вольт-амперні характеристики при освітленні для кожного типу сонячних елементів. Встановлено, що найбільше значення коефіцієнта корисної дії сонячних елементів з подвійним $n\text{-i-p}$ -гетеропереходом у разі освітлення з інтенсивністю 100 мВт/см^2 площі елементів 1 см^2 становить $11,5\%$.